Why trait gradients across environments differ within species and across communities: Insights from a theoretical model

Sophie Yang[1*], William K. Cornwell[1], Isaac R. Towers[1], Daniel S. Falster[1]

[1]Evolution & Ecology Research Centre, University of New South Wales

[*]**Corresponding author:** sophie.yang@unsw.edu.au

Keywords: abundant-centre hypothesis, competition, dispersal, evolution, gene swamping, genetic variation, microclimate, migration load, natural selection, trait-based ecology.

Word count: 4949

Acknowledgements

This research was supported by the Commonwealth through an Australian Government Research Training Program Scholarship [DOI: https://doi.org/10.82133/C42F-K220]. Travel and support for DSF, IRT and SY were funded by an Australian Research Council Discovery Project (DP240100177). IRT was also funded by an Australian Research Council Linkage Project (LP230100049). We thank the Cornster Lab for their warm feedback and support. Open access publishing was facilitated by the University of New South Wales, as part of the The Royal Society Open Access Publishing Agreement.

Declaration of AI use

Artificial intelligence (AI) was used to assist the development of code, improve readability of this work, and as a search engine. The authors take full responsibility for the content of the work.

1 Abstract

Trait-environment relationships within plant species are both flatter on average and more variable than community-mean trends, yet the mechanisms driving this variation remain poorly understood. Classic theory attributes this flattening to maladaptive gene flow, but the theory has been underused and its scope, in particular how multiple factors interact to shape trait slopes, remains largely unexplored. Here, we extend it: we model a multi-species community along a one-dimensional environmental gradient to test how four factors shape adaptation within species through time. We found genetic variance accelerated adaptation and steepened trait slopes, while higher gene flow and steeper environmental gradients slowed adaptation and flattened within-species slopes, compared to optimal or across-species responses. Micro-environmental heterogeneity produced flatter slopes without the density penalty imposed by gene flow. The same dynamics governing trait adaptation also govern species abundance distributions; we show abundant-centre patterns are not a general expectation, but a signal of incomplete adaptation. These results connect eco-evolutionary theory to the empirical literature on within-species trait variation, providing a mechanistic basis for interpreting trait slopes and abundant-centre patterns across environmental gradients.

2 Introduction

A fundamental observation since the beginning of ecology has been the shift in the form and function of living things along environmental gradients [1, 2]. Broadly, plant species are known to shift in their functional traits (traits that impact growth, survival and/or reproduction) and gradually be replaced by other species as environmental conditions change across space [2, 3, 4, 5]. Despite significant progress in quantifying the rates of trait and species turnover along environmental gradients [e.g., 6, 7, 8, 9], the degree to which traits shape species distributions remains poorly understood.

Existing theory offers a promising but underused hypothesis: that species' trait-environment slopes —

and ultimately their distributions — are shaped by the interplay of adaptation and gene flow, which operates differently within species than across communities. Imagine there is an optimal phenotype (trait value) that shifts along space. One might expect species to adapt perfectly to this environmental gradient by matching their traits to the optimum (Fig. 1a). Classic theory suggests, however, that a single species cannot fully track a shifting optimum because gene flow from differing environments continuously pulls trait means away from local optima — a process known as maladaptive gene flow or migration load (Fig. 1b) [10, 11, 12, 13, 14]. Along a linear environmental gradient, abundance differences across space result in asymmetric gene flow and hence a net flow of maladaptive genes into lower-density populations [12]. The interplay of both maladaptive gene flow and competition with other species along environmental gradients can thereby flatten species' trait slopes and ultimately promote species turnover along the gradient [13].

The empirical record broadly supports the outcome of the proposed gene flow effect: the flattening of within-species trait slopes compared to community-mean slopes. Although there is some variation, empirical data show that the changes in trait values along environmental gradients are typically smaller within species, compared to the changes averaged across whole communities (Fig. 1c) [15, 4, 16, 17, 18, 19]. For example, Cornwell and Ackerly [4] found strong positive trends in leaf area and specific leaf area along a gradient of soil water content in coastal California; however, the distribution of within-species trait-environment slopes was shallower than the community-mean slope. Consequently, the community-level trend was driven largely by species replacement, rather than within-species trait variation. This was corroborated by Guo, Cornwell, and Bragg [19], who found that leaf area-precipitation relationships in the eucalypt clade were weaker at shallow phylogenetic scales, primarily within species. But, despite this consistent average pattern, within-species slopes vary considerably [20, 19]; what drives that variation, and how trait responses connect to adaptation and species turnover, remains unresolved.

Despite mounting empirical evidence on within-species trait slopes, the ability of original theory to explain variation in trait slopes has been underused. Analysis by Case and Taper [13] showed that gene flow can flatten trait gradients, contributing to turnover, but focused only on two species. It

is unclear whether other factors modulate the degree of flattening, whether these processes scale to repeated turnover of multiple species, or what happens if a location supports more than one optimal phenotype. Moreover, Case and Taper [13] assumed reduced competition through trait divergence, but given that trait-based competition does not apply well to plants competing for common resources [21], can trait-independent competition for resources also generate flatter trait gradients? A few theoretical studies have observed flatter trait slopes in passing; however, results have been centred on other processes and phenomena, making it difficult to disentangle the effects of each driver [e.g., 22]. Thus it remains unclear what factors are most important in shaping the observed shallowness and variability in within-species trait slopes.

While untested, existing theory suggests several predictions about within-species trait slopes. Higher genetic variance should steepen slopes, by increasing the capacity and rate of local adaptation [12, 13]. Higher dispersal rates and steeper environmental gradients are each expected to increase migration load (the fitness loss when individuals move among locally-adapted populations), thereby flattening slopes [12, 13]. Spatial heterogeneity at the local scale ('micro-environments') should introduce additional axes of trait variation that decouple within-species slopes from the large-scale gradient, generating greater variability across species [23, 24, 25].

The same dynamics governing trait adaptation along gradients also determine how species abundance varies across space. This connects directly to the abundant-centre hypothesis—the proposition that species reach peak abundance at the centre of their range and decline toward the edges [26, 27]—which has attracted substantial empirical attention but remains unresolved, partly because empirical tests have proceeded largely without mechanistic theory to interpret them [28, 29, 30, 31]. Population density in classic models is jointly controlled by selection, gene flow and competition, so the same simulations yield predictions about both trait slopes and abundance distributions—offering a mechanistic basis for interpreting when and why abundant-centre patterns should or should not emerge.

Here, we extend the classic two-species model of Case and Taper [13] to a multi-species community, and test whether gene flow and adaptation can generate the observed variety of within-species trait

slopes, even with trait-independent competition. Specifically, we ask how four factors shape within-species trait-environment slopes compared to cross-community responses: genetic variance, which theory predicts should steepen slopes by accelerating local adaptation; dispersal rate and gradient steepness, each expected to flatten slopes by increasing migration load and suppressing edge densities; and local spatial heterogeneity (micro-environments), which should flatten slopes without the density costs that dispersal imposes. Because population density emerges directly from these dynamics, the same simulations generate predictions about species abundance distributions, including when and why abundant-centre patterns should arise.

3 Methods

To investigate these questions, we model the eco-evolutionary dynamics of a community along a one-dimensional environmental gradient (Fig. 2). We begin with a scenario where each location along the gradient has a unique optimal trait value, before extending the model to accommodate multiple optima at each location.

In the single optimum case, we consider the population density $N_i(x,t)$ and trait mean $\bar{z}_i(x,t)$ for a species i at location x in space and time t, in a community comprising of S species. We consider a species as a group of individuals connected by gene flow, regardless of phenotypic divergence (i.e. intraspecific variation) across space. We define z to be a one-dimensional phenotypic trait. We assume that there is an optimum trait value z^* at any location, which varies through space x and is fixed through time t (Fig. 2). The model is based on standard equations that incorporate local physiological fitness, Lotka-Volterra competition, directional selection and gene flow, following Kirkpatrick and N. H. Barton [12] and Case and Taper [13] but without trait-based competition coefficients (see below).

We assume species i has a distribution of trait values (i.e. phenotypes) that vary with space x and time

t, with mean $\bar{z}_i(x,t)$ and a distribution of $p_i(z,x,t)$ within any location, such that

$$\int p_i(z,x,t)\,dz = 1, \tag{1}$$

and

$$\int z\,p_i(z,x,t)\,dz = \bar{z}_i(x,t). \tag{2}$$

The local distribution $p_i(z,x,t)$ is assumed to follow a normal distribution with variance V, which remains constant across space x and time t, such that

$$p_i(z,x,t) = p_i(z). \tag{3}$$

Let $w(z,x,t)$ be the per capita growth rate for phenotype z at x and t. We let w vary as

$$w\,(z,x,t) = r(z,x,t) - \sum_j N_j(x,t) \int p_j(z')\;\alpha(z,z')\,dz'. \tag{4}$$

The potential per-capita growth rate $r(z,x,t)$ is allowed to vary with distance from an optimal trait value $z^*(x,t)$ as

$$r(z,x,t) = r_0 \exp\left(-\frac{(z^*(x,t)-z)^2}{\sigma^2}\right) - \kappa, \tag{5}$$

where r_0 is the maximum intrinsic growth rate, σ^2 is the width of the response of potential per-capita growth rate to divergence from $z^*(x,t)$ and κ is the intrinsic mortality parameter.

We model competition as a fixed per capita reduction in $w(z,x,t)$ with the abundance of competitors (denoted as species j), i.e.,

$$\alpha(z,z') = a_0. \tag{6}$$

Following Norberg et al. [22], we assume that competition does not depend on the difference in trait values between individuals, given that trait-based competition functions do not apply well to plants competing for common resources [21]. Thus, all individuals compete fully with all others in a patch.

By definition, the average per capita growth rate w for species i is given by

$$\bar{w}_i(x,t) = \int p_i(z)\, w(z,x,t)\, dz. \tag{7}$$

Individuals disperse according to a diffusion process, with dispersal rate D [Fick's second law; 32].

The change in population density over time is then given by

$$\underbrace{\frac{\partial N_i(x,t)}{\partial t}}_{\substack{\text{change in} \\ \text{population}}} = \underbrace{N_i(x,t)\ \bar{w}_i(x,t)}_{\text{population dynamics}} + \underbrace{D\frac{\partial^2 N_i}{\partial x^2}(x,t)}_{\text{dispersal}}, \tag{8}$$

while the change in mean trait value is given by

$$\underbrace{\frac{\partial \bar{z}_i}{\partial t}(x,t)}_{\substack{\text{change in} \\ \text{mean trait}}} = \underbrace{N_i(x,t)\ V\frac{\partial w}{\partial z}(z,x,t)\bigg|_{z=\bar{z}_i(x,t)}}_{\text{directional selection}} + \underbrace{D\left(\frac{\partial^2 \bar{z}_i}{\partial x^2}(x,t) + 2\frac{\partial \log N_i(x,t)}{\partial x}\ \frac{\partial \bar{z}_i}{\partial x}(x,t)\right)}_{\text{gene flow}}. \tag{9}$$

We assume that the rate of directional selection is proportional to genetic variance V and the size of the population $N_i(x,t)$ [33], such that directional selection stalls when population size is low.

3.1 Multiple trait optima at each location

We introduce multiple optima to the model, to capture the scenario where each location x along the gradient has multiple 'micro-environments'. Trait optima of different micro-environments all shift linearly at the same rate but are offset from one another by a specified amount (Fig. 2). In this multi-optima model, the change in population density of species i in micro-environment m is given

by

$$\underbrace{\frac{\partial N_{i,m}}{\partial t}(x,t)}_{\substack{\text{change in}\\ \text{population}}} = \underbrace{N_{i,m}(x,t)\,\bar{w}_{i,m}(x,t)}_{\text{population dynamics}} + \underbrace{D\frac{\partial^2 N_{i,m}}{\partial x^2}(x,t)}_{\text{dispersal across space}} + \underbrace{\sum_{m=0}^{M-1}\frac{\beta}{M-1}(N_{i,m'}(x,t) - N_{i,m}(x,t))}_{\text{movement among micro-environments}}, \tag{10}$$

where M is the total number of micro-environments, β is the exchange rate of individuals between micro-environments ($1/\text{time}$) and m' is another micro-environment in the given location x. The change in mean trait value in micro-environment m over time is likewise given by

$$\begin{aligned}\underbrace{\frac{\partial \bar{z}_{i,m}}{\partial t}(x,t)}_{\substack{\text{change in}\\ \text{mean trait}}} = {} & \underbrace{N_{i,m}(x,t)\,V\frac{\partial w}{\partial z}(z,x,t)\Big|_{z=\bar{z}_{i,m}}}_{\text{directional selection}} + \underbrace{D\left(\frac{\partial^2 \bar{z}_{i,m}}{\partial x^2}(x,t) + 2\frac{\partial \log N_{i,m}}{\partial x}(x,t)\frac{\partial \bar{z}_{i,m}}{\partial x}(x,t)\right)}_{\text{gene flow across space}} \\ & + \underbrace{\sum_{m=0}^{M-1}\frac{\beta}{M-1}\,\frac{N_{i,m'}(x,t)}{N_{i,m}(x,t)}\,(\bar{z}_{i,m'}(x,t) - \bar{z}_{i,m}(x,t))}_{\text{gene flow among micro-environments}},\end{aligned} \tag{11}$$

where $N_{i,m'}$ is the number of immigrants from micro-environment m' and $N_{i,m}$ is the local density.

3.2 Numerical implementation

To implement the model described above, we focus on dynamics of the trait means $\bar{z}_i(x,t)$ and population densities $N_i(x,t)$.

Based on a second-order Taylor expansion [22], $\bar{w}_i(x,t)$ can be approximated as

$$\bar{w}_i(x,t) = w\left(\bar{z}_i(x,t), x, t\right) + \frac{1}{2}V\frac{\partial^2 w}{\partial z^2}(z,x,t)\Big|_{z=\bar{z}_i(x,t)}. \tag{12}$$

The second term gives the average increase or decrease in per capita growth rate that arises through non-linearity in $w(z)$.

The first derivative, $\frac{\delta w}{\delta z}$, can be solved to give

$$\frac{\delta w}{\delta z}(z,x,t)\bigg|_{z=\bar{z}_i(x,t)} = \frac{2r_0(z^*(x,t)-z)}{\sigma^2}\exp\left(\frac{-(z^*(x,t)-z)^2}{\sigma^2}\right). \tag{13}$$

The second derivative can be solved to give

$$\frac{\delta^2 w}{\delta z^2}(z,x,t)\bigg|_{z=\bar{z}_i(x,t)} = \frac{2r_0}{\sigma^2}\exp\left(\frac{-(z^*(x,t)-\bar{z}_i(x,t))^2}{\sigma^2}\right)\left(\frac{2(z^*(x,t)-\bar{z}_i(x,t))^2}{\sigma^2}-1\right). \tag{14}$$

To solve this model numerically, we consider K nodes along space x. At each node k, we approximate the density N_i and mean trait value $\bar{z}_i$ of each species i. Species' genetic variances V and dispersal rates D are fixed parameters.

Under the multiple optima framework, we designate M micro-environments at every node k, which are offset by a fixed parameter, such that they shift linearly and at the same rate across space.

For numerical stability and to prevent densities becoming negative during numerical approximation, we tracked the change in the natural logarithm of population density $\log(N_i(x,t))$ rather than $N_i(x,t)$, using the identity

$$\frac{\delta \log(N_i(x,t))}{\delta t} = \frac{\delta N_i(x,t)}{\delta t}\frac{1}{N_i(x,t)}. \tag{15}$$

We also apply an upper limit to population density to counter numerical instability at the boundaries of space. We set the derivative $\frac{\delta \log(N_i(x,t))}{\delta t}$ to zero if $\log(N_i(x,t)) + \Delta\log(N_i(x,t))$ was to exceed the minimum of two logistic curves:

$$\min\left(\frac{10}{1+e^{-s(x-x_A)}}, \frac{10}{1+e^{s(x-x_B)}}\right), \tag{16}$$

where s is the steepness of the logistic curves and x_A and x_B are the left and right midpoints of the curves respectively. $\Delta\log(N_i(x,t))$ is calculated by multiplying $\frac{\delta \log(N_i(x,t))}{\delta t}$ by Δt, with $\Delta t = 1$. The midpoints x_A and x_B are set by a parameter X (a proportion of total space multiplied by the number of nodes K) designating their distances from the edges of space. We multiply the curves by a factor of 10 so that the maximum density cutoff in the centre of the space is not too restrictive but still provides

numerical stability. We also limit further decreases in population density if already too low, by setting $\frac{\delta \log(N_i(x,t))}{\delta t}$ to zero if $\log(N_i(x,t)) < \log(0.00001)$ and $\frac{\delta \log(N_i(x,t))}{\delta t} < 0$.

Parameters and their default values are described in Table S1.

At initial conditions (time = 0), all species were at maximum density across space (and across micro-environments under the multiple optima framework). Trait means were also fixed across space, evenly spaced between minimum and maximum values of the environmental gradient. We allowed a 'warm-up' period from time = 0 to time = 100, with V and D parameters set to zero, such that there was no evolution or dispersal during this period. During the warm-up period, species sorted across space to where their trait means were closest to the optimum. After the warm-up period, V and D were increased to specified values.

4 Results

We found that higher genetic variance (V) accelerated adaptation, increasing within-species trait slopes at time = 200, as predicted (Fig. 3). Dispersal rate (D) had the opposing effect: increased gene flow homogenised trait means across space, thereby suppressing population density at range edges and increasing overlap among species distributions. Under high gene flow, the system reached a steady state more slowly, with trait slopes remaining flat through a balance of selection and gene flow (Fig. 3c). Genetic variance had a stronger overall effect than dispersal rate; dispersal rate required an increase by several orders of magnitude to exert a comparable influence.

Steeper environmental gradients produced results similar to higher dispersal (Fig. 4). Sharper changes in the optimum among neighbouring locations increased mismatches between trait means and the optima, except at the range centres, suppressing population densities (Fig. 4a). Under the example parameterisation, all simulations eventually reached steady states, but more slowly under steeper gradients, as the gaps between initial trait slopes and the environmental gradient were larger (Fig.

4b).

Adding micro-environments with different trait optima within each location resulted in overall flatter within-species trait slopes, compared to a single optimum in each location (Fig. 5). Instead of adapting to the environmental slope, species were able to switch to another optimum partway through space for which they were already pre-adapted. When not at steady state and with large distances among optima (time = 1000, Fig. 5a), the addition of a third optimum flattened within-species trait slopes even more than the presence of two optima, such that the overall within-species trait slope was approximately zero. This was caused by the sharp negative transitions of trait means as species shifted optima, in contrast to the overall positive environmental slope. Multiple optima also enabled local coexistence. When optima were far apart, each species occupied the micro-environment it was best adapted to, and multiple species coexisted at every location. When optima were close, each species dominated all micro-environments within its range core, with trait means averaged across optima, while coexisting with other species at the range periphery.

Abundance distribution shapes depended on how closely within-species trait slopes matched the environmental gradient (Fig. 3). Poorly adapted species—with flat trait slopes—had hump-shaped distributions, consistent with the abundant-centre hypothesis. At steady state, fully-adapted species had uniform distributions with sharp boundaries between species, counter to the hypothesis. Distribution shape thus tracked the same factors governing trait slope steepness: genetic variance, dispersal rate, gradient steepness, and time for adaptation.

In simulations with a single optimum per location, within-species trait slopes were linear, except under simultaneously high genetic variance and dispersal rate, where they became S-shaped, with adaptation of edge populations lagging behind the range core (Figs. 3, 4). With multiple optima, trait means were non-linear and disjointed across geographic space, especially at steady state (Fig. 5); however, they became approximately linear when plotted against environmental space (Fig. 6).

5 Discussion

Here, we revive classic eco-evolutionary models [12, 13] to investigate the degree to which traits influence species' distributions. Our results partition the contributions of intraspecific trait variation versus species turnover to community assembly along environmental gradients. The model suggests intraspecific trait variation is a function of the level of adaptation to an environmental gradient, which is governed by combined effects of time, gene flow, genetic variance, and microsite diversity. Consistent with studies modelling the effects of climate change on biodiversity [22, 34], we found that genetic variance accelerated adaptation, leading to steeper trait slopes, whereas dispersal rate and gene flow slowed adaptation, leading to shallower trait slopes and suppressed population densities at range edges. We also demonstrated a previously unexplored mechanism for flattening species trait slopes without the density penalty: micro-environmental heterogeneity. When species are not fully adapted to the gradient (at disequilibrium), such as with strong gene flow, trait values along the gradient are controlled primarily by across-species turnover rather than within-species trait variation. Our paper highlights a neglected opportunity for a bridge between the theoretical and empirical literature surrounding problems of adaptation and species distributions.

With the rise of trait-based ecology comes discourse about the relative importance of intraspecific trait variation [35]. Empirical data shows trait-environment relationships are, on average, flatter within species than across communities [15, 4, 17, 18, 19]. This aligns with global findings by Siefert et al. [16] that intraspecific trait variation and species turnover account for 32% and 64% of total community-level trait variation, respectively. In other words, trait change along gradients primarily results from species turnover. Our model links intraspecific trait variation to the degree of species' adaptation to environmental gradients, thereby affecting their trait-environment slopes, and provides mechanisms to explain the relative importance of within-species variation and turnover in the assembly of communities along environmental gradients.

We demonstrated the influence of three factors that control species' adaptation to an environmental gradient: genetic variance, dispersal rate and gradient steepness. As expected, genetic variance (the

amount of genetic variation available for natural selection to act upon) accelerated adaptation to the gradient, leading to steeper slopes and higher intraspecific trait variation (Fig. 3). Since genetic variance is simply a term that modulates the strength of directional selection in the model, it could be equally regarded as the effect of generation time, which is negatively correlated with the potential rate of evolution [36], or any other drivers of genetic variation [37]. Conversely, gene flow homogenised trait values across space, slowing adaptation to the gradient. The empirical data aligns with either a non-equilibrial state—species are in the process of adapting—or with the outcome of the gene flow effect [15, 4, 17, 18, 19]: gene flow reduces the signal of the environment in within-species trait variation, producing flatter within-species trait slopes on average. Although dispersal can sometimes be beneficial for species' persistence under environmental change [38, 39], gene flow as a homogenising force suggests adept dispersers might adapt more slowly to environmental gradients [40]. Future empirical work could investigate whether dispersal syndrome predicts species' trait-environment slopes. Further, the maladaptation induced by steeper gradients and higher gene flow led to suppressed population densities away from species' range centres. Although community assembly processes (e.g., migration and speciation) are not encoded in our model, these vacancies in carrying capacity imply that better-adapted species could invade; steeper environmental gradients and high-dispersal taxa should therefore display higher turnover. This matches rapid turnover rates observed along steep elevational gradients [2, 41, 42].

Collectively, the factors we explored control the rate of adaptation and, ultimately, the time required for the system to reach equilibrium, by modulating the relative influences of natural selection and gene flow. The timeline of our simulations, from initial conditions to steady state, parallels the arrival of species to a new environmental gradient and the subsequent adaptation via evolution to the gradient. A striking empirical example of this process is the spectacular radiation of the Hawaiian lobeliads: after colonising the archipelago, the group diversified into many distinct habitat types with associated traits [43, 44]. Corroborating our findings, limited dispersal in the largest lobeliad genus *Cyanea* likely accelerated adaptive radiation independently across the islands [44]. Trait-environment slopes observed today are snapshots of systems that may or may not have reached equilibrium. Our results suggest that when species are not yet fully adapted (at disequilibrium), or when gene flow is sufficiently strong,

trait turnover is primarily driven by across-species turnover rather than intraspecific trait variation. The empirical finding that trait gradients are generally flatter within species than across communities, and that turnover outweighs intraspecific trait variation [4, 16], is consistent with the view that many systems remain at disequilibrium.

The connection of traits to species distributions forms an underappreciated bridge between theoretical and empirical research. Classic eco-evolutionary theory [11, 12, 13], although highly stylised, still offers underexploited heuristic value. In particular, it presents mechanisms to predict range sizes and species turnover rates, a focal goal of empirical investigation [45, 46]. A central assumption of early models is a single continuously shifting optimum along one dimension [12, 13, 47]. Here, we revive classic models with a simple yet illuminating extension: the addition of multiple optima to represent micro-environmental heterogeneity in nature. Superimposed on macro-scale environmental gradients, local-scale heterogeneity is influenced by, among other things, topography and vegetation feedbacks which manifest as shaded understories to exposed sun-facing slopes [48, 49, 50]. Persistent micro-environments have been recognised as important refugia for species when the surrounding climatic conditions become unsuitable [23, 24, 25]. Given the option of multiple trait optima, our model showed that species switched among optima across space, rather than evolving to match the overall environmental slope, leading to flatter within-species trait slopes but without the density penalty associated with gene flow. This also opened the opportunity for the coexistence of different phenotypes in each location. Empirical data shows within-species and across-community trait-environment relationships tend to vary in the same direction [4, 16]; however, our model does not account for the occasional reversal—species trait slopes opposing the environmental gradient [20, 19]. Additionally, questions remain about how much micro-environmental heterogeneity exists relative to macro-environmental gradients and how heterogeneity is distributed across local scales. These present opportunities for further empirical investigation.

Discrepancies between a model and empirical data can arise because the empirical system in question does not match model assumptions, or because the model misses relevant biological processes for that system [51, 30]. The abundant-centre hypothesis (that species should be most abundant in the centres

of their distribution) [26, 27] is an example of where the theoretical basis has been largely ignored in empirical investigations [28, 29, 30, 31]. Abundant-centre patterns have emerged from models that assume a monotonic environmental gradient such as ours [12, 13], but environmental space and geographic space are not always well correlated in reality [52, 51, 53, 29]. Abundance distributions in our simulations ranged from hump-shaped, as predicted by the hypothesis, to uniform, counter to the hypothesis. The shapes of the distributions depended on the same factors that governed trait adaptation, suggesting that abundant-centre patterns are not a general expectation, but an indicator of incomplete adaptation [14]. We predict that better dispersers are slower to adapt to environmental gradients due to increased migration load [40], which aligns with the finding that greater dispersal ability appears correlated with decreased genetic differentiation among populations [54]. Due to incomplete adaptation, we predict better dispersers will more often exhibit abundant-centre distributions. The increased maladaptation toward peripheral populations experienced by stronger dispersers, and along steeper gradients, might also facilitate greater coexistence.

Finally, we offer some recommendations for better integrating theory and observation. Although mechanistic theory has historically been underused in interpreting empirical findings, efforts to do so are steadily growing [55, 29, 30]. We urge empiricists to consider the assumptions underlying hypotheses like the abundant centre, and particularly the contexts in which certain patterns are expected to emerge. For theoreticians, models should connect explicitly to measurable functional traits to enable empirical validation. Though this proved useful as a minimal demonstration that a small set of processes can generate diverse within-species trait-environment slopes, future modelling could incorporate explicit resources, trait-based trade-offs and lifespan [56, 57]. The integration of observation and theory is crucial to all sciences; ecology is no exception [58]—and that integration is best served not by conceptual frameworks alone, but by quantitative models precise enough to be meaningfully tested against data [59]. On that, we all have more work to do.

5.1 Conclusions

We have shown that the flatness and variability of within-species trait-environment slopes, long noted empirically but poorly explained, emerge here from a small set of interacting processes along environmental gradients: selection, gene flow, competition, and local spatial heterogeneity. Critically, the same dynamics that govern trait slopes determine the shapes of species abundance distributions, offering a mechanistic basis for interpreting when abundant-centre patterns should and should not arise. These findings generate concrete, testable predictions: species with greater genetic variance should adapt faster and thereby have steeper trait slopes; species with higher dispersal should show flatter trait slopes and more hump-shaped abundance distributions; steeper environmental gradients should produce greater turnover; and local micro-environmental heterogeneity should decouple within-species slopes from community-mean trends without the density costs imposed by gene flow. Connecting these predictions to empirical data, particularly the growing availability of intraspecific trait databases, is a worthy next step toward a unified account of how traits, adaptation and species distributions are linked across environmental gradients.

References

1. Schimper A. F. W. Pflanzen-geographie auf physiologischer Grundlage. Jena: Gustav Fischer, 1898

2. Humboldt A. v. and Bonpland A. Essai sur la géographie des plantes: accompagné d'un tableau phyqique des régions équinoxiales, fondé sur des mesures exécutées, depuis le dixième degré de latitude boréale jusqu'au dixième degré de latitude australe, pendant les années 1799, 1800, 1801, 1802 et 1803. Paris: Levrault & Schoell, 1805

3. Reich P. B., Wright I. J., Cavender-Bares J., Craine J. M., Oleksyn J., Westoby M., and Walters M. B. The evolution of plant functional variation: Traits, spectra, and strategies. International Journal of Plant Sciences. 2003; 164(S3):S143–S164. DOI: 10.1086/374368

4. Cornwell W. K. and Ackerly D. D. Community assembly and shifts in plant trait distributions across an environmental gradient in coastal California. Ecological Monographs. 2009; 79:109–26. DOI: 10.1890/07-1134.1

5. Towers I. R., Vesk P. A., Wenk E. H., Gallagher R. V., Windecker S. M., Wright I. J., and Falster D. S. Revisiting the role of mean annual precipitation in shaping functional trait distributions at a continental scale. New Phytologist. 2024; 241:1900–9. DOI: 10.1111/nph.19478

6. Harrison S., Ross S. J., and Lawton J. H. Beta diversity on geographic gradients in Britain. Journal of Animal Ecology. 1992; 61:151–8. DOI: 10.2307/5518

7. Qian H. and Ricklefs R. E. A latitudinal gradient in large-scale beta diversity for vascular plants in North America. Ecology Letters. 2007; 10:737–44. DOI: 10.1111/j.1461-0248.2007.01066.x

8. Fitzpatrick M. C., Sanders N. J., Normand S., Svenning J.-C., Ferrier S., Gove A. D., and Dunn R. R. Environmental and historical imprints on beta diversity: insights from variation in rates of species turnover along gradients. Proceedings of the Royal Society B: Biological Sciences. 2013; 280:20131201. DOI: 10.1098/rspb.2013.1201

9. Ulrich W., Soliveres S., Maestre F. T., Gotelli N. J., Quero J. L., Delgado-Baquerizo M., Bowker M. A., Eldridge D. J., Ochoa V., Gozalo B., Valencia E., Berdugo M., Escolar C., García-Gómez M., Escudero A., Prina A., Alfonso G., Arredondo T., Bran D., Cabrera O., Cea A. P., Chaieb M., Contreras J., Derak M., Espinosa C. I., Florentino A., Gaitán J., Muro V. G., Ghiloufi W., Gómez-González S., Gutiérrez J. R., Hernández R. M., Huber-Sannwald E., Jankju M., Mau R. L., Hughes F. M., Miriti M., Monerris J., Muchane M., Naseri K., Pucheta E., Ramírez-Collantes D. A., Raveh E., Romão R. L., Torres-Díaz C., Val J., Veiga J. P., Wang D., Yuan X., and Zaady E. Climate and soil attributes determine plant species turnover in global drylands. Journal of Biogeography. 2014; 41:2307–19. DOI: 10.1111/jbi.12377

10. Haldane J. B. S. The relation between density regulation and natural selection. Proceedings of the Royal Society of London Series B - Biological Sciences. 1956; 145:306–8. DOI: 10.1098/rspb.1956.0039

11. García-Ramos G. and Kirkpatrick M. Genetic models of adaptation and gene flow in peripheral populations. Evolution. 1997; 51:21–8. DOI: 10.1111/j.1558-5646.1997.tb02384.x

12. Kirkpatrick M. and Barton N. H. Evolution of a species' range. The American Naturalist. 1997; 150:1–23. DOI: 10.1086/286054

13. Case T. J. and Taper M. L. Interspecific competition, environmental gradients, gene flow, and the coevolution of species' borders. The American Naturalist. 2000; 155:583–605. DOI: 10.1086/303351

14. Polechová J. Is the sky the limit? On the expansion threshold of a species' range. PLOS Biology. 2018; 16. Ed. by Jordano P.:e2005372. DOI: 10.1371/journal.pbio.2005372

15. Ackerly D. D., Knight C., Weiss S., Barton K., and Starmer K. Leaf size, specific leaf area and microhabitat distribution of chaparral woody plants: contrasting patterns in species level and community level analyses. Oecologia. 2002; 130:449–57. DOI: 10.1007/s004420100805

16. Siefert A., Violle C., Chalmandrier L., Albert C. H., Taudiere A., Fajardo A., Aarssen L. W., Baraloto C., Carlucci M. B., Cianciaruso M. V., L. Dantas V. de, Bello F. de, Duarte L. D. S., Fonseca C. R., Freschet G. T., Gaucherand S., Gross N., Hikosaka K., Jackson B., Jung V., Kamiyama C., Katabuchi M., Kembel S. W., Kichenin E., Kraft N. J. B., Lagerström A., Bagousse-

Pinguet Y. L., Li Y., Mason N., Messier J., Nakashizuka T., Overton J. M., Peltzer D. A., Pérez-Ramos I. M., Pillar V. D., Prentice H. C., Richardson S., Sasaki T., Schamp B. S., Schöb C., Shipley B., Sundqvist M., Sykes M. T., Vandewalle M., and Wardle D. A. A global meta-analysis of the relative extent of intraspecific trait variation in plant communities. Ecology Letters. 2015; 18:1406–19. DOI: 10.1111/ele.12508

17. Libalah M. B., Droissart V., Sonké B., Hardy O. J., Drouet T., Pescador D. S., Kenfack D., Thomas D. W., Chuyong G. B., and Couteron P. Shift in functional traits along soil fertility gradient reflects non-random community assembly in a tropical African rainforest. 2017; 150:265–78. DOI: 10.5091/plecevo.2017.1318

18. Taseski G. M., Keith D. A., Dalrymple R. L., and Cornwell W. K. Shifts in fine root traits within and among species along a fine-scale hydrological gradient. Annals of Botany. 2021; 127:473–81. DOI: 10.1093/aob/mcaa175

19. Guo K., Cornwell W. K., and Bragg J. G. Using machine learning to link climate, phylogeny and leaf area in eucalypts through a 50-fold expansion of leaf trait datasets. Journal of Ecology. 2024; 112:2183–97. DOI: 10.1111/1365-2745.14354

20. Dong N., Prentice I. C., Evans B. J., Caddy-Retalic S., Lowe A. J., and Wright I. J. Leaf nitrogen from first principles: field evidence for adaptive variation with climate. Biogeosciences. 2017; 14:481–95. DOI: 10.5194/bg-14-481-2017

21. Falster D. S., Kunstler G., FitzJohn R. G., and Westoby M. Emergent shapes of trait-based competition functions from resource-based models: a Gaussian is not normal in plant communities. The American Naturalist. 2021; 198:253–67. DOI: 10.1086/714868

22. Norberg J., Urban M. C., Vellend M., Klausmeier C. A., and Loeuille N. Eco-evolutionary responses of biodiversity to climate change. Nature Climate Change. 2012; 2:747–51. DOI: 10.1038/nclimate1588

23. Lenoir J., Hattab T., and Pierre G. Climatic microrefugia under anthropogenic climate change: implications for species redistribution. Ecography. 2017; 40:253–66. DOI: 10.1111/ecog.02788

24. McLaughlin B. C., Ackerly D. D., Klos P. Z., Natali J., Dawson T. E., and Thompson S. E. Hydrologic refugia, plants, and climate change. Global Change Biology. 2017; 23:2941–61. DOI: 10.1111/gcb.13629

25. Kerr J. T., Gordon S. C. C., Chen I.-C., Ednie G., Foden W., Newbold T., Reynolds A. R., Suggitt A. J., Terblanche J. S., and Watson M. J. Effects of microclimate variation on insect persistence under global change. Nature Reviews Biodiversity. 2025; 1:532–42. DOI: 10.1038/s44358-025-00067-4

26. Brown J. H. On the relationship between abundance and distribution of species. The American Naturalist. 1984; 124:255–79. DOI: 10.1086/284267

27. Sagarin R. D. and Gaines S. D. The 'abundant centre' distribution: to what extent is it a biogeographical rule? Ecology Letters. 2002; 5:137–47. DOI: 10.1046/j.1461-0248.2002.00297.x

28. Santini L., Pironon S., Maiorano L., and Thuiller W. Addressing common pitfalls does not provide more support to geographical and ecological abundant-centre hypotheses. Ecography. 2019; 42:696–705. DOI: 10.1111/ecog.04027

29. Feng X. and Qiao H. Accounting for dispersal using simulated data improves understanding of species abundance patterns. Global Ecology and Biogeography. 2022; 31:200–14. DOI: 10.1111/geb.13412

30. Maitra A., Pandit R., Mungee M., and Athreya R. Testing a theoretical framework for the environment-species abundance paradigm: a new approach to the Abundant Centre Hypothesis. 2022. DOI: 10.1101/2022.01.03.474819

31. Panter C. T., Kambach S., Bachman S. P., Baines O., Bruelheide H., Sporbert M., Hähn G. J. A., Field R., and Schrodt F. Plants with higher dispersal capabilities follow 'abundant-centre' distributions but such patterns remain rare in animals. Nature Communications. 2025; 16:8205. DOI: 10.1038/s41467-025-63566-0

32. Fick A. Ueber diffusion. Annalen der physik. 1855; 170:59–86

33. Dieckmann U. and Law R. The dynamical theory of coevolution: a derivation from stochastic ecological processes. Journal of Mathematical Biology. 1996; 34:579–612. DOI: 10.1007/BF02409751

34. Åkesson A., Curtsdotter A., Eklöf A., Ebenman B., Norberg J., and Barabás G. The importance of species interactions in eco-evolutionary community dynamics under climate change. Nature Communications. 2021; 12:4759. DOI: 10.1038/s41467-021-24977-x

35. Westerband A. C., Funk J. L., and Barton K. E. Intraspecific trait variation in plants: A renewed focus on its role in ecological processes. Annals of Botany. 2021; 127:397–410. DOI: 10.1093/aob/mcab011

36. Lewin L. and Eyre-Walker A. Estimates of the mutation rate per year can explain why the molecular clock depends on generation time. Molecular Biology and Evolution. 2025; 42:msaf069. DOI: 10.1093/molbev/msaf069

37. Crow J. F. and Kimura M. An introduction to population genetics theory. Harper & Row, 1970

38. Loreau M., Mouquet N., and Gonzalez A. Biodiversity as spatial insurance in heterogeneous landscapes. Proceedings of the National Academy of Sciences. 2003; 100:12765–70. DOI: 10.1073/pnas.2235465100

39. Román-Palacios C. and Wiens J. J. Recent responses to climate change reveal the drivers of species extinction and survival. Proceedings of the National Academy of Sciences. 2020; 117:4211–7. DOI: 10.1073/pnas.1913007117

40. Lenormand T. Gene flow and the limits to natural selection. Trends in Ecology & Evolution. 2002; 17:183–9. DOI: 10.1016/S0169-5347(02)02497-7

41. Rahbek C., Borregaard M. K., Colwell R. K., Dalsgaard B., Holt B. G., Morueta-Holme N., Nogues-Bravo D., Whittaker R. J., and Fjeldså J. Humboldt's enigma: What causes global patterns of mountain biodiversity? Science. 2019; 365:1108–13. DOI: 10.1126/science.aax0149

42. McFadden I. R., Sandel B., Tsirogiannis C., Morueta-Holme N., Svenning J.-C., Enquist B. J., and Kraft N. J. Temperature shapes opposing latitudinal gradients of plant taxonomic and phylogenetic β diversity. Ecology Letters. 2019; 22:1126–35. DOI: 10.1111/ele.13269

43. Givnish T. J. Adaptive radiation, dispersal, and diversification of the Hawaiian lobeliads. *The Biology of Biodiversity*. Ed. by Kato M. Tokyo: Springer Japan, 2000 :67–90. DOI: 10.1007/978-4-431-65930-3_5

44. Givnish T. J., Millam K. C., Mast A. R., Paterson T. B., Theim T. J., Hipp A. L., Henss J. M., Smith J. F., Wood K. R., and Sytsma K. J. Origin, adaptive radiation and diversification of the Hawaiian lobeliads (Asterales: Campanulaceae). Proceedings of the Royal Society B: Biological Sciences. 2009; 276:407–16. DOI: 10.1098/rspb.2008.1204

45. Lester S. E., Ruttenberg B. I., Gaines S. D., and Kinlan B. P. The relationship between dispersal ability and geographic range size. Ecology Letters. 2007; 10:745–58. DOI: 10.1111/j.1461-0248.2007.01070.x

46. Soininen J. Species turnover along abiotic and biotic gradients: Patterns in space equal patterns in time? BioScience. 2010; 60:433–9. DOI: 10.1525/bio.2010.60.6.7

47. Alleaume-benharira M., Pen I. R., and Ronce O. Geographical patterns of adaptation within a species' range: interactions between drift and gene flow. Journal of Evolutionary Biology. 2006; 19:203–15. DOI: 10.1111/j.1420-9101.2005.00976.x

48. Aguiar M. R. and Sala O. E. Patch structure, dynamics and implications for the functioning of arid ecosystems. Trends in Ecology & Evolution. 1999; 14:273–7

49. Rietkerk M., Ketner P., Burger J., Hoorens B., and Olff H. Multiscale soil and vegetation patchiness along a gradient of herbivore impact in a semi-arid grazing system in West Africa. Plant Ecology. 2000; 148:207–24. DOI: 10.1023/A:1009828432690

50. Geiger R., Aron R. H., and Todhunter P. The climate near the ground. Bloomsbury Publishing PLC, 2009

51. Pironon S., Papuga G., Villellas J., Angert A. L., García M. B., and Thompson J. D. Geographic variation in genetic and demographic performance: new insights from an old biogeographical paradigm. Biological Reviews of the Cambridge Philosophical Society. 2017; 92:1877–909. DOI: 10.1111/brv.12313

52. Sagarin R. D., Gaines S. D., and Gaylord B. Moving beyond assumptions to understand abundance distributions across the ranges of species. Trends in Ecology & Evolution. 2006; 21:524–30. DOI: 10.1016/j.tree.2006.06.008

53. Bontrager M., Usui T., Lee-Yaw J. A., Anstett D. N., Branch H. A., Hargreaves A. L., Muir C. D., and Angert A. L. Adaptation across geographic ranges is consistent with strong selection in marginal climates and legacies of range expansion. Evolution. 2021; 75:1316–33. DOI: 10.1111/evo.14231

54. Bohonak A. J. Dispersal, gene flow, and population structure. The Quarterly Review of Biology. 1999; 74:21–45

55. Dallas T. A. and Santini L. The influence of stochasticity, landscape structure and species traits on abundant–centre relationships. Ecography. 2020; 43:1341–51. DOI: 10.1111/ecog.05164

56. Falster D. S., FitzJohn R. G., Brännström Å., Dieckmann U., and Westoby M. plant: A package for modelling forest trait ecology and evolution. Methods in Ecology and Evolution. 2016; 7:136–46. DOI: 10.1111/2041-210X.12525

57. Falster D. S., Duursma R. A., and FitzJohn R. G. How functional traits influence plant growth and shade tolerance across the life cycle. Proceedings of the National Academy of Sciences. 2018; 115:E6789–E6798. DOI: 10.1073/pnas.1714044115

58. Rastetter E. B. Modeling for understanding v. modeling for numbers. Ecosystems. 2017; 20:215–21. DOI: 10.1007/s10021-016-0067-y

59. Marquet P. A., Allen A. P., Brown J. H., Dunne J. A., Enquist B. J., Gillooly J. F., Gowaty P. A., Green J. L., Harte J., Hubbell S. P., O'Dwyer J., Okie J. G., Ostling A., Ritchie M., Storch D., and West G. B. On theory in ecology. BioScience. 2014; 64:701–10. DOI: 10.1093/biosci/biu098

6 Figures and Tables

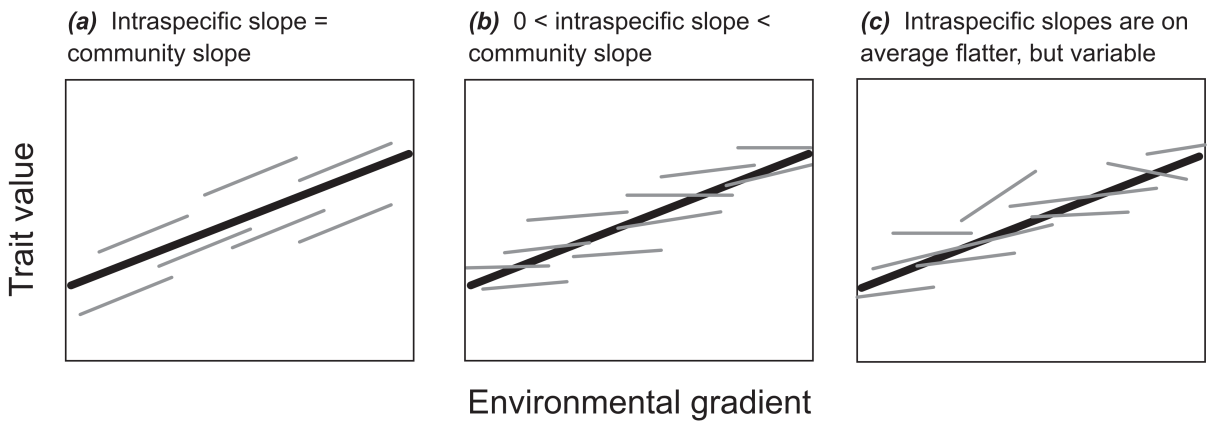

311 **Figure 1.** Three scenarios for within-species (grey lines) and across-community (black lines) trait slopes along
312 an environment gradient. (a) The null expectation is that species are able to perfectly track the environmental
313 gradient across space. (b) However, theory suggests maladaptive gene flow produces flatter within-species trait
314 slopes, with shifts in trait values across space driven mainly by turnover of species, rather than intraspecific
315 trait variation. (c) Empirical data shows that within-species trait slopes are on average flatter than the across-
316 community trait slope, albeit exhibiting considerable variation. This figure was inspired by Cornwell and Ackerly
317 [4].

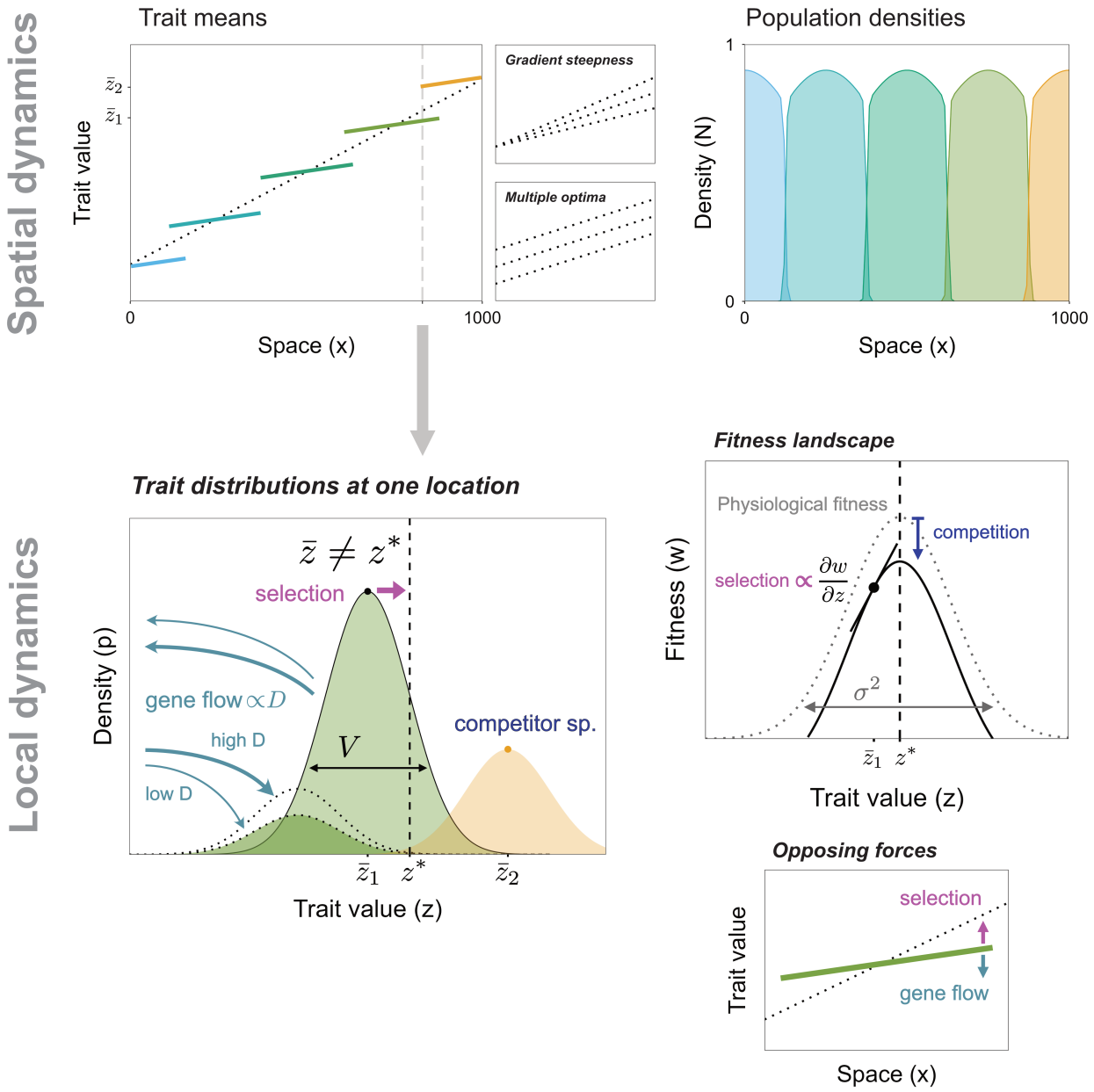

Figure 2. Spatial eco-evolutionary dynamics of five species (different coloured lines) as encoded by the model. The assumed optimum trait value(s) is indicated by the dotted line, with options to increase the steepness of the optimum gradient or introduce multiple optima per location. Species' trait means and population densities are distributed across one-dimensional space. At each location (one example indicated by the vertical dashed line), trait means evolve under forces of selection towards the assumed optimum and gene flow from other locations. Gene flow moves from both neighbouring locations, often asymmetrically—here, it occurs on one side for demonstration purposes only. Physiological fitness, controlled by the distance between a species' trait mean and the local optimum, is reduced by competition to give fitness (w). Selection is proportional to the steepness of the fitness landscape ($\frac{\partial w}{\partial z}$). Under the multiple optima framework, species are able to migrate among micro-environments with different optima.

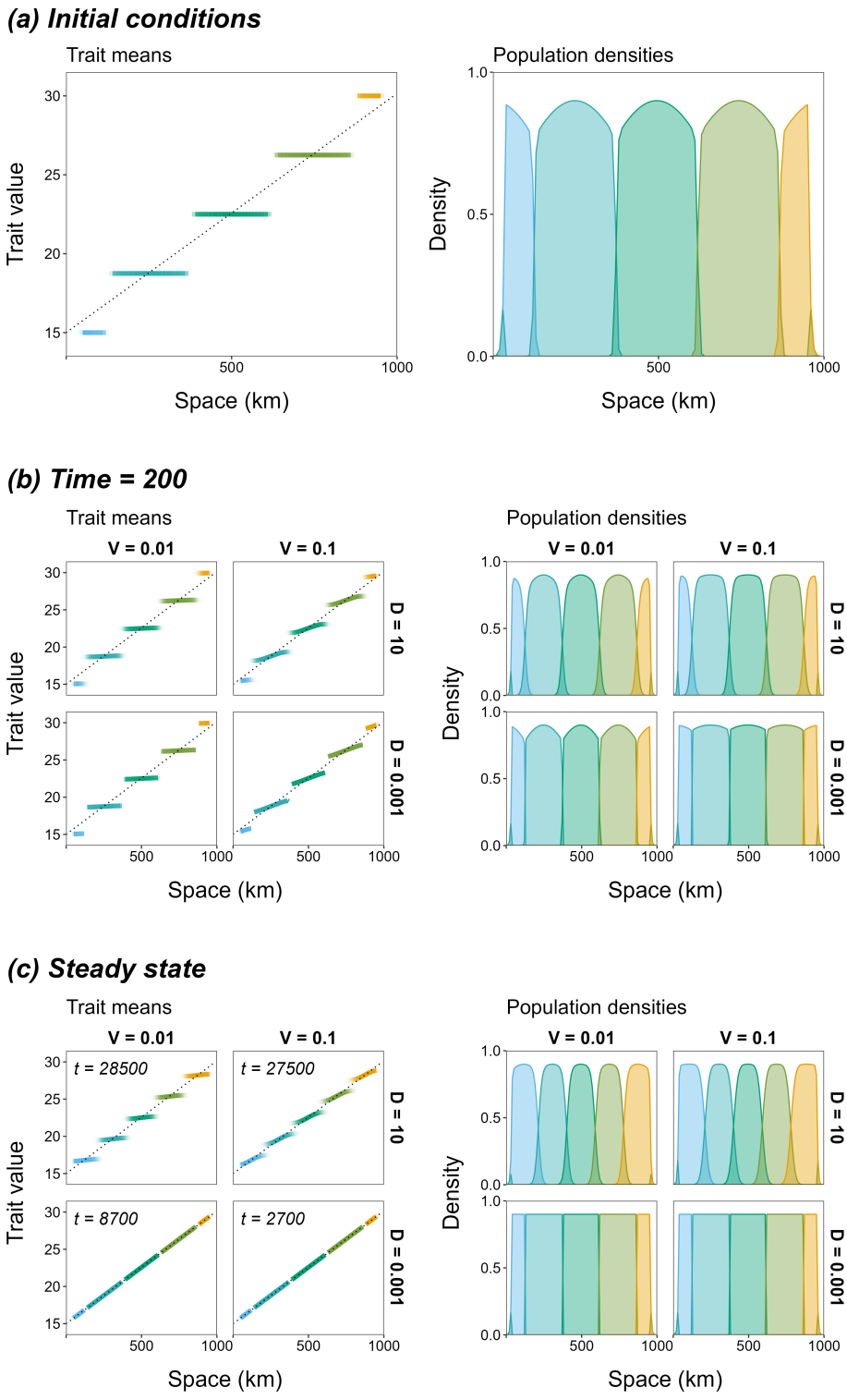

Figure 3. The effect of average genetic variance (V) and dispersal rate (D) on species trait slopes and abundance distributions across space at various time points. The dotted lines represent the assumed optimal trait values across space. (a) The initial conditions of each simulation after the warm-up period (time = 100), with all species (different coloured lines) at equilibrial densities before any evolution or dispersal. (b) The states of the system under varying V and D parameterisations, at time = 200. (c) The steady states of the system under the same parameterisations. 'Steady state' was defined as the state at which the rates of change of abundance-weighted trait means were under 1×10^{-4}, checked at time intervals of 200. Other parameters are described in Table S1.

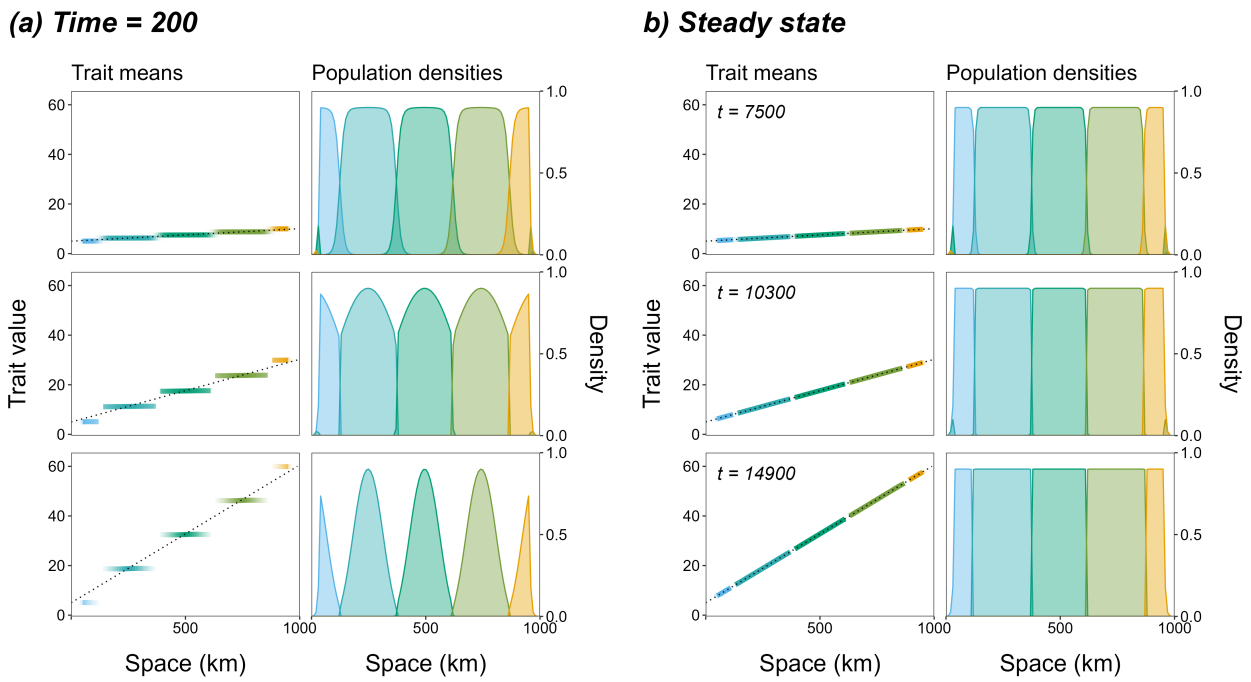

Figure 4. The effect of gradient steepness on the pattern and rate of adaptation to the environmental gradient. The dotted lines represent the assumed optimum trait values across space. (a) The states of the system at time = 200 and (b) the steady states of the system, under varying steepness. 'Steady state' was defined as the state at which the rates of change of abundance-weighted trait means were under 1×10^{-4}, checked at time intervals of 200. The initial conditions of every simulation are as described in Fig. 3a (but initial trait means were evenly spread between the minimum and maximum optimum values across space, differing with gradient steepness). V and D were set to 0.01 and K was set to 200. Other parameters are described in Table S1.

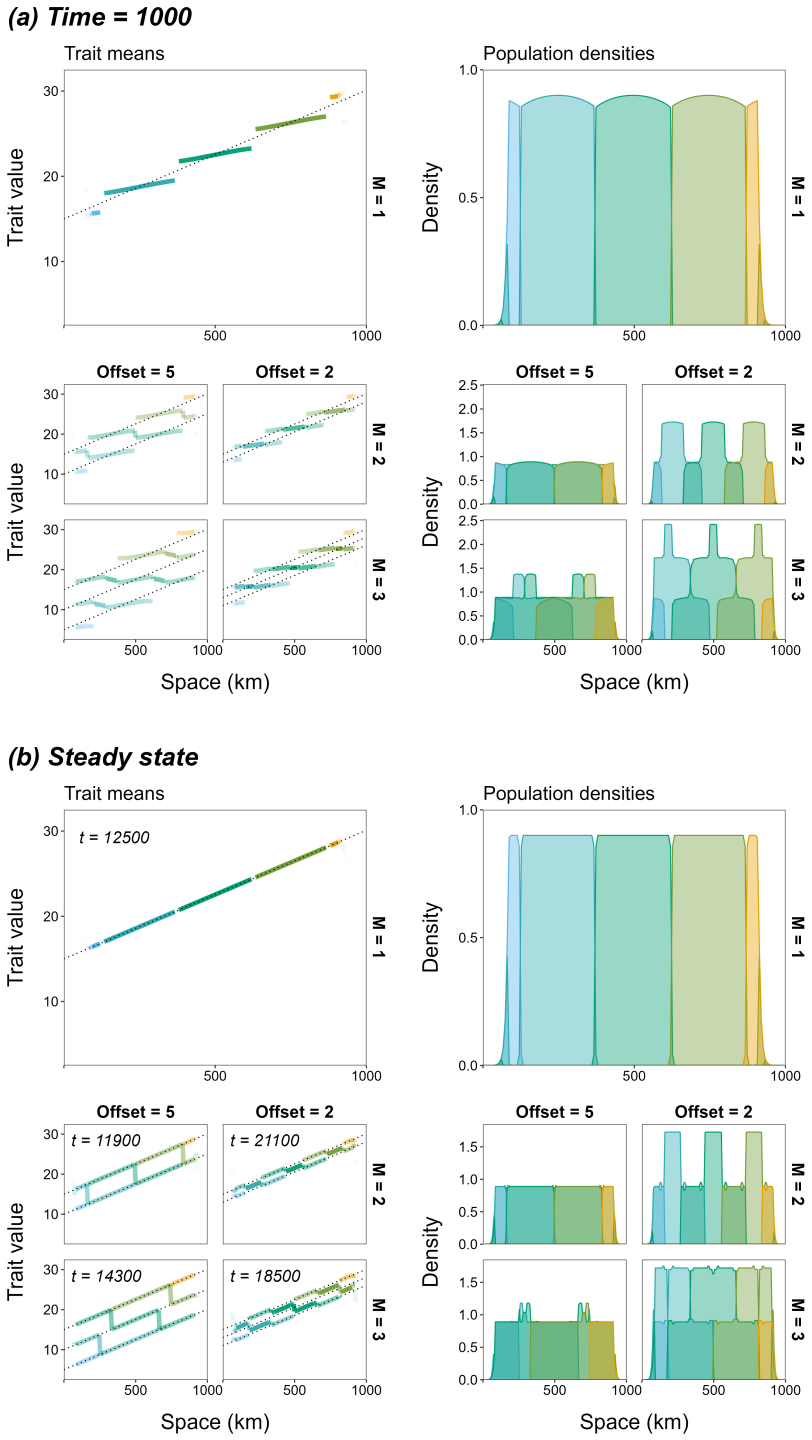

Figure 5. The pattern of adaptation across space comparing a single optimum versus multiple optima within each location, with the latter akin to local micro-environments with different optimal trait values. The trait optima are represented by the dotted lines. (a) The states at time = 1000 and (b) the steady states of the system for different numbers of optima per location (M) and distances among optima ('offset'). 'Steady state' was defined as the state at which the rates of change of abundance-weighted trait means were under 1×10^{-4}, checked at time intervals of 200. For simulations with multiple optima, trait means are averaged and population densities are summed across micro-environments. At initial conditions (time = 100), species reach constant densities across micro-environments and space, before any evolution or dispersal. V, D, and K were set to 0.01, 0.001, and 150 respectively. For increased numerical stability, we changed s and X to 1 and 0.2 respectively. Other parameters are described in Table S1.

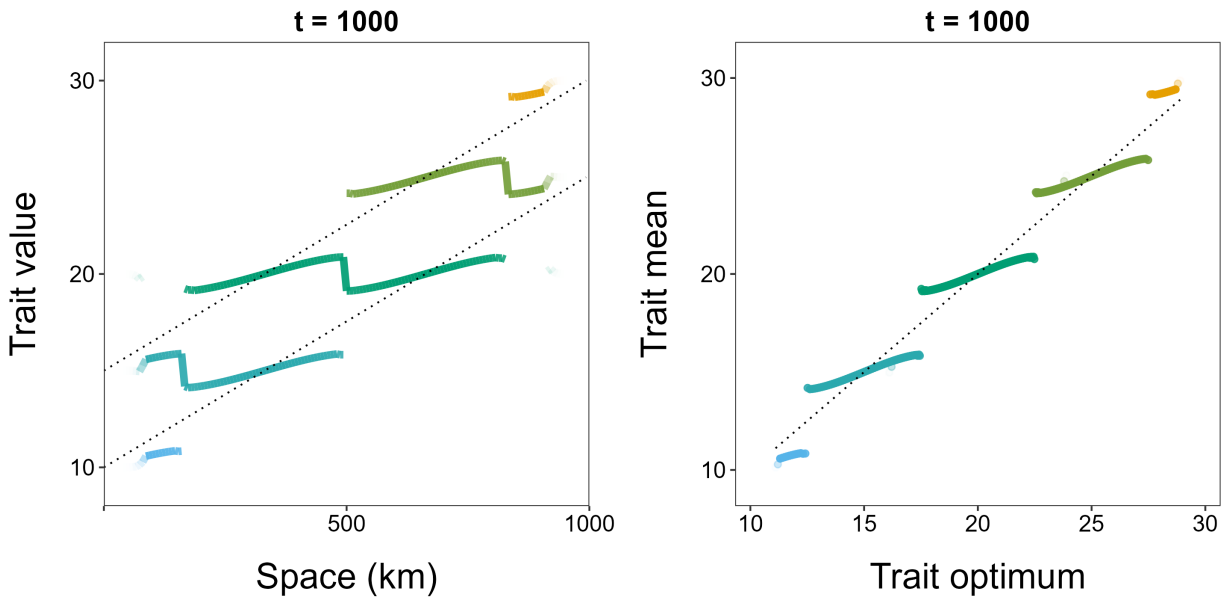

Figure 6. Comparison of the pattern of adaptation across geographic space (left) and environmental space (right) at time = 1000 for a simulation with multiple optima. Parameters are as described in Fig. 5, with $M = 2$ and Offset $= 5$. Species trait means were plotted as points against environmental trait optima. Only points where population density was greater than 0.1 were included.

7 Supplementary materials

Table S1. Model parameters and default values (if applicable).

Number of species	S	5
Number of nodes	K	100
Number of micro-environments	M	
Average genetic variance	V	
Average dispersal rate	D	
Intrinsic growth rate	r_0	1
Width of the maximum growth rate response	σ^2	25
Intrinsic mortality parameter	κ	0.1
Competition coefficient	a_0	1
Movement rate between micro-environments	β	0.01
Steepness of density-limiting logistic curves	s	2
Proportion of space to set midpoints of density-limiting logistic curves	X	0.1